A NUMERICAL SIMULATION OF THE ADVECTIVE AND DIFFUSIVE TRANSFER OF TRACE SUBSTANCES IN THE STRATOSPHERE

Hugh Edward Willoughby

United States Naval Postgraduate School

THESIS

A NUMERICAL SIMULATION OF THE ADVECTIVE AND DIFFUSIVE TRANSFER OF TRACE SUBSTANCES IN THE STRATOSPHERE

by

Hugh Edward Willoughby

December 1969

A Numerical Simulation of the Advective and Diffusive Transfer of Trace Substances in the Stratosphere

by

Hugh Edward Willoughby
Lieutenant (junior grade), United States Navy
B.S., University of Arizona, 1967

Submitted in partial fulfillment of the
requirements for the degree of

MASTER OF SCIENCE IN METEOROLOGY

from the

NAVAL POSTGRADUATE SCHOOL
December 1969

ABSTRACT

A numerical model which employes observed stratospheric winds to advect simulated tracers was developed. This model successfully reproduces many qualitative features of the observed fields of both ozone and radioactive debris. As the tracers evolve, the horizontal eddies constitute the principal process modifying the tracer zonal mean. Although the vertical eddies and the zonal mean cell are both an order of magnitude weaker than this process, the latter of these tends to always act in the same sense so that its effect becomes more important over long periods of time.

TABLE OF CONTENTS

LIST OF FIGURES

LIST OF SYMBOLS

b_1-b_6	Ratio of the time-step to the corresponding characteristic time
b_7	Ratio of the advection time to the diffusion time
$f(m^{\ell},\omega^{\ell},u^{\ell},v^{\ell})$	A function representing the derivative of mixing ratio due to the combined effects of diffusion and advection
i	Lattice index corresponding to pressure
j	Lattice index corresponding to latitude
k	Lattice index corresponding to longitude
K_1	Vertical eddy diffusivity
K_2	Horizontal eddy diffusivity
ℓ,n	Lattice indices corresponding to time
m	Tracer mixing-ratio
$\overline{m}$	Local mean m
m*	Departure of m from $\overline{m}$
$m^n_{i,j,k}$	Value of m at a lattice point (i,j,k,n)
p	Pressure
R	Earth's radius
t	Time
u	Zonal wind velocity
v	Meridional wind velocity
x^n	Dummy variable in time integration
δt	Time step
δp	Pressure increment
$\delta \phi$	Latitude increment
$\delta \lambda$	Longitude increment

ϕ	Latitude
λ	Longitude
τ_1	Vertical advection time
τ_2	Meridional advection time
τ_3	Zonal advection time
τ_4	Vertical diffusion time
τ_5	Meridional diffusion time
τ_6	Zonal diffusion time
ω	Vertical motion in pressure coordinates = $\frac{dp}{dt}$
ω_o, u_o, v_o	Non-dimensionalizing constants for the wind velocities
$\bar{\omega}, \bar{u}, \bar{v}$	Local mean wind velocities
ω^*, u^*, v^*	Departures of the wind velocities from the local mean
$\breve{\omega}, \breve{u}, \breve{v}$	Zonal mean wind velocities
ω', u', v'	Non-dimensionalized wind velocities
ω'', u'', v''	Wind field with natural zonal mean replaced by an arbitrary zonal mean
$\omega^n_{i,j,k}, u^n_{i,j,k}$ $v^n_{i,j,k}$	Non-dimensionalized wind field tabulated at a lattice point (i,j,k,n)
Ω, v	Arbitrary zonal mean v and ω

ACKNOWLEDGEMENT

The author wishes to express his gratitude to Professor Jerry D. Mahlman for making his wind data available as well as for his help, advice and constructive criticism during the formulation and execution of this research; and to Professor R. T. Williams for his suggestions concerning the manuscript. Thanks also to Mr. James Cerullo and Mr. Michael McDermet for drafting the figures, the Computer Facility at the Naval Postgraduate School for its assistance with the numerical computations, and to Miss Barbara Smith and Mrs. Sara Anderson who typed the manuscript.

I. BACKGROUND

A. OBSERVATIONS

The study of trace substance transport in the stratosphere can provide many useful insights into the dynamics of that region. The history of an evolving inert tracer depends upon its initial state and upon several statistical properties of the wind field. In the stratosphere, detailed observations of the wind field are not always plentiful enough to reveal these rather subtle characteristics of the general circulation. In addition to observations of the wind, there exist some observations of the distributions of such natural tracers as ozone and radioactive debris. These observations may be used to extend the available data base, and theories of the general circulation may be tested by requiring them to simulate the advection of natural tracers.

The influence of stratospheric transport processes was first noticed when the early spectrophotometer observations of Dobson and his co-workers (Dobson et al. 1928) revealed that the distribution of total atmospheric ozone has the following characteristics:

1. The total amount of ozone per unit area increases from the equator toward the poles.

2. In high latitudes this quantity varies with season exhibiting a pronounced maximum in late winter or early spring.

3. No apparent correlation exists between total ozone and solar activity.

4. Total ozone is correlated with the passage of upper-level synoptic systems, attaining positive departures from its long-term mean in the lows and negative departures in the highs.

Dobson's observations are consistent with those obtained by the 81 station network in the Soviet Union and reported by Bozkov (1968). These observations indicate that:

1. Minimum total ozone occurs at 10 N.

2. Maximum total ozone occurs at 60 to 70 N, with values decreasing toward both the equator and the pole.

3. The maximum zonal mean gradient of total ozone occurs between 30 and 60 N.

4. The total ozone tends to have a wavelike distribution in the horizontal with low values occurring over the western portions of continents and high values over the eastern portions.

The photochemical theory of ozone formation (See Craig, 1965) predicts that, at photochemical equilibrium, the distribution of total ozone should attain a maximum in low latitudes at the subsolar point and increase toward the poles. Brewer (1949) and Dobson (1956) attempt to reconcile this theory with observation by postulating a mean cell with ascending motion in low latitudes, northward advection in the high mid-latitude stratosphere, descent near the pole, and a return circulation at low levels in mid-latitudes. This circularion supposedly carries the ozone, which is generated by solar ultraviolet radiation in low latitudes, northward and downward into the lower polar stratosphere where it accumulates since there it is protected from photodissociation.

The Brewer-Dobson theory is seriously challenged by airborne filter observation of the distribution of Tungsten-185 from the Hardtack nuclear tests (Feely and Spar, 1960). The center of concentration of this debris remained at 50 mb and nearly at the latitude of injection. The cloud did not migrate northward and downward, but rather spread in the meriodinal plane

in such a manner that the isopleths of concentration sloped downward from the equator toward the pole.

B. PARAMETERIZED MODELS

Reed (1950) and Normand (1953) note that stratospheric troughs are regions of both high temperature and high total ozone. This leads them to postulate that, since both potential temperature and ozone mixing ratio increase upward, the lows must be regions of descending motion and the highs regions of ascent. Furthermore, the troughs and ridges move more slowly than the wind so that horizontal advection shifts the centers of greatest mixing-ratio departure downwind from the associated pressure system. Because the wind almost always has a westerly component in the winter season, the ozone maxima lie in the southerly winds east of the troughs and the minima are east of the ridges in northerly winds. Thus, the departures of both temperature and mixing-ratio are explained in terms of the systematic interaction between horizontal and vertical advection. High mixing-ratio and temperature is accompanied by descent and poleward motion while low values of these two quantities occur with rising and equatorward motion.

Citing earlier work by Dodson (1960), Newell (1961) carries this line of reasoning one step further. He explains the poleward slope of the isopleths by invoking eddy mixing in which northward motion is correlated with descent and southward motion with ascent. In the same paper he computes the flux of ozone by correlating total ozone with the winds at 12-18 km in the maximum ozone layer. He finds that 90 percent of his computed flux is due to large-scale eddies and that the total flux is more than adequate to explain observed changes in the distribution.

Prabhakara (1961) generates zonal mean ozone distributions which depend upon the interaction of photochemistry, a mean cell that descends near the pole, and large-scale eddies parameterized as anisotropic diffusion. His results, which are in good qualitative agreement with observation,show that such transport processes can explain many departures from photochemical equilibrium.

In contrast to Prabhakara's work, in which the principal axis of eddy diffusion is horizontal, there have been a number of models simulating the transport of radioactive debris with anisotropic diffusion schemes in which the principal axis is inclined to the horizontal (Reed and German, 1965; Davidson, et al., 1965; Seitz, et al., 1968; and Fairhall and Reed, 1968). In such models it is assumed that the northward-downward velocity correlation in the large-scale eddies can be parameterized in terms of a diffusion tensor whose principal axis slopes downward toward the pole. This means that the tracer is presented with a path of least resistance parallel to the observed slope of the isopleths of mixing ratio in the real atmosphere. In order to keep the tracer on these sloping paths and to prevent excessive vertical spreading, it is necessary to make the vertical component of the diffusion tensor much smaller than that along the principal axis. Davidson et al. (1966) use a principal diffusivity of 4×10^9 cm^2 sec^{-1} and a vertical diffusivity of about $10^4 cm^2$ sec^{-1}. However, since characteristic horizontal distances are on the order of 10^3 km while vertical distances are about 1 km and, since the speed of diffusion depends upon the square of these distances, a ratio of 10^6 between the two diffusivities is not physically unreasonable.

C. GENERAL CIRCULATION MODELS

Hunt and Manabe (1968) and Hunt (1969) report the most extensive and realistic simulation of stratospheric tracers to date. In their experiments various simulated substances are introduced into the wind fields generated by a general circulation model and the history of the numerically evolved mixing ratio fields are examined.

In the 1968 experiments inert tracers are permitted to evolve from zonally symmetric initial states. The first such tracer roughly corresponds to radioactive debris from an equatorial injection and is initially distributed in a band extending from the equator to ten degrees north with the maximum concentration at 50 mb pressure height.

The second experiment's initial state represents the distribution of ozone at photochemical equilibrium throughout the region of integration. Both tracers are treated as inert substances inasmuch as, except for removal of any tracer that finds its way into the troposphere, no sources or sinks are included in these experiments.

The simulated histories of both tracers are reassuringly similar to observations of real tracers in the atmosphere. Both the radioactive debris and the ozone begin at once to migrate northward and, to some extent, downward. Thus the concentration at the equator decreases and that at the poles increases, so that the initial gradient becomes smaller and eventually reverses.

The actual transfer by the quasi-horizontal eddies is well illustrated by the evolution of the mixing ratio field at various horizontal levels in the model. The zonally symmetric character of the initial field quickly disappears becoming sinusoidal with wave number four predominating as it does in the circulation generated by the model. With the passage of time

the waves becomes increasingly exaggerated, forming the mixing-ratio contours into long northward protrusions. Eventually the protrusions separate, leaving isolated islands of high concentration in northern latitudes.

Hunt (1969) reports two additional experiments with the same model and involving ozone transport with photochemical sources and sinks added. The mechanism of transfer in these studies and in those previously discussed are very similar. In both, the mean cell, which produces a convergence of tracer into the subtropics, is opposed by an eddy divergence out of that region, with the eddies being particularly effective in transferring tracer northward in the region poleward of 30N. The principal difference introduced by photochemistry is the strong source in low latitudes which prevents reduction or reversal of the initial poleward gradient by replacing the ozone as fast as transport processes can remove it.

The weak link in any experiment involving either parameterization or a general circulation model lies in the arbitrary specification of the transport process and its, at best, indirect relation to the actual motions in the stratosphere. In view of these difficulties, it seems instructive to compare advection of simulated tracers by actual observed winds with both observation and previous attempts to model both ozone and radioactive debris. The present study, therefore, employs actual observed stratospheric winds to advect simulated tracers in the presence of sub-grid-scale diffusion and numerically integrates the equation of continuity for the tracer in time to obtain the evolution of an inert tracer from an arbitrary initial state.

This approach is largely independent of any preconceived ideas about the stratospheric general circulation and so provides a third source of information intermediate between the parameterized models or the general circulation models and observations of real tracers.

II. MODEL

A. BASIC EQUATION

The present study follows the lead of Hunt and Manabe (1968) by numerically exploring the detailed advection of trace substances without resort to arbitrarily defined diffusion tensors. Furthermore, the winds used to accomplish this advection are based on actual observations of the real atmosphere and are not the result of a mathematical model that may or may not reproduce the properties of the actual general circulation.

The basic equation on which this study depends is the equation of continuity for an inert tracer without sources or sinks, expressed in flux form and spherical pressure coordinates.

$$-\frac{\partial m}{\partial t} = \frac{\partial}{\partial p}(m\omega) + \frac{1}{R\cos\phi}\frac{\partial}{\partial\phi}mv\cos\phi + \frac{1}{R\cos\phi}\frac{\partial}{\partial\lambda}mu \quad , \qquad (1)$$

where m is the mixing ratio of the tracer, R the earth's radius, ϕ the geographic latitude, λ the longitude, p the pressure, ω the substantial pressure derivative following an individual air parcel, and u and v the wind's eastward and northward components respectively.

The local mean of any dependent variable in (1) is defined as its average computed over a volume characteristic of the grid distance to be used in the integration. The value at any point within the region can now be represented by the sum of this mean and a departure from the mean

$$m = \bar{m} + m^* \qquad u = \bar{u} + u^*$$
$$v = \bar{v} + v^* \qquad \omega = \bar{\omega} + \omega^* \,, \tag{2}$$

where the starred variables are the departures and the barred ones are the means. These relations are then substituted into (1) and the entire relation is averaged recognizing that, while the average of a fluctuation alone or of the product of a fluctuation with a mean vanish, the averaged product of two fluctuations does not. (See Haltiner & Martin, 1957).

$$-\frac{\partial \bar{m}}{\partial t} = \frac{\partial}{\partial p}(\bar{m}\bar{\omega}) + \frac{1}{R\cos\phi}\left\{\frac{\partial}{\partial \phi}(\bar{m}\bar{v}\cos\phi) + \frac{\partial}{\partial \lambda}(\bar{m}\bar{u})\right\}$$
$$+ \frac{\partial}{\partial p}(\overline{m^*\omega^*}) + \frac{1}{R\cos\phi}\left\{\frac{\partial}{\partial \phi}(\overline{m^*v^*}\cos\phi) + \frac{\partial}{\partial \lambda}(\overline{m^*u^*})\right\}. \tag{3}$$

The terms containing products of fluctuations are then approximated by using the Prandtl mixing-length assumption that the correlation between velocity and mixing-ratio is proportional to the mean gradient of mixing ratio as given by

$$\overline{m^*\omega^*} = -K_1\frac{\partial \bar{m}}{\partial p} \qquad \overline{m^*v^*} = -\frac{K_2}{R}\frac{\partial \bar{m}}{\partial \phi}$$
$$\overline{m^*u^*} = -\frac{K_2}{R\cos\phi}\frac{\partial \bar{m}}{\partial \lambda}. \tag{4}$$

The vertical and horizontal eddy diffusivities, K_1 and K_2 are assumed to be constant in both space and time. This particular choice of constants, with the same eddy diffusivity in both horizontal directions and without any off-diagonal elements in the diffusivity tensor, implies that diffusion is isotropic in the horizontal plane with the axis of least diffusion oriented vertically since $K_1 \ll K_2$.

By substituting (4) for the eddy correlation terms in (3) and writing the flux terms back in advective form through use of the mass continuity equation for the local mean flow, one obtains

$$-\frac{\partial \bar{m}}{\partial t} = \bar{\omega}\frac{\partial \bar{m}}{\partial p} + \frac{\bar{v}}{R}\frac{\partial \bar{m}}{\partial \phi} + \frac{\bar{u}}{R\cos\phi}\frac{\partial \bar{m}}{\partial \lambda}$$

$$-K_1\frac{\partial^2 \bar{m}}{\partial p^2} - \frac{K_2}{R^2\cos\phi}\frac{\partial}{\partial \phi}\left(\cos\phi\frac{\partial \bar{m}}{\partial \phi}\right) - \frac{K_2}{R\cos^2\phi}\frac{\partial^2 \bar{m}}{\partial \lambda^2}. \qquad (5)$$

At this point (5) is placed in non-dimensionalized form by the following linear transformation of the velocity fields:

$$\bar{u} = u_0 u', \quad \bar{v} = v_0 v', \quad \bar{\omega} = \omega_0 \omega'. \qquad (6)$$

Here the sub-zero values are constants with magnitudes ($u_0 = v_0 = 20$ kt, $\omega_0 = 5$ mb day^{-1}) so chosen that the primed variables, whose variations contain the spatial and temporal changes of the velocities, are of order one. Since the equation is linear in $\bar{m}$ no such scaling needs to be done for thatvariable and (5) becomes

$$-\frac{\partial \bar{m}}{\partial t} = \omega_0\omega'\frac{\partial \bar{m}}{\partial p} + \frac{v_0 v'}{R}\frac{\partial \bar{m}}{\partial \phi} + \frac{u_0 u'}{R\cos\phi}\frac{\partial \bar{m}}{\partial \lambda}$$

$$-K_1\frac{\partial^2 \bar{m}}{\partial p^2} - K_2\left\{\frac{1}{R^2\cos\phi}\frac{\partial^2 \bar{m}}{\partial \phi^2} + \frac{1}{R^2\cos^2\phi}\frac{\partial^2 \bar{m}}{\partial \lambda^2}\right\} \qquad (7)$$

For solution on a digital computer the infinitesimal derivativies in (7) have to be replaced by finite differences, thus converting the partial differential equation into a system of algebraic equations in the mixing ratio and wind components at discrete points in the region of integration. This procedure requires that the independent variables of the problem be expressed as multiples of small but finite increments so that the coordinates of a point (p, ϕ, λ, t) become i,j,k and n; where $i = p/\delta p$, $j = (\phi - \phi_0)/\delta\phi$, $k = \lambda/\delta\lambda$ and $n = t/\delta t$ and the values assumed by (p, ϕ, λ, t) are required to make i, j, k and n integers. In this formalism $\bar{m}(p,\phi,\lambda, t)$ is $m^n_{i,j,k}$ and $v(p,\phi,\lambda, t)$ is $v^n_{i,j,k}$.

Once such a coordinate system is set up it becomes possible to approximate the time derivative by a forward difference

$$\frac{\partial \bar{m}}{\partial t} = \frac{m^{n+1}_{i,j,k} - m^{n}_{i,j,k}}{\delta t} , \tag{8}$$

the first order space derivatives by centered differences, for example,

$$\frac{\partial \bar{m}}{\partial p} = \frac{m^{n}_{i+1,j,k} - m^{n}_{i-1,j,k}}{2\delta p} = \frac{\Delta_i m^n}{2\delta p} , \tag{9}$$

and to use the three point approximation in place of the second order space derivatives

$$\frac{\partial^2 \bar{m}}{\partial p^2} = \frac{m^{n}_{i+1,j,k} - 2m^{n}_{i,j,k} + m^{n}_{i-1,j,k}}{(\delta p)^2} = \frac{\Delta_i^2 m^n}{(\delta p)^2} . \tag{10}$$

The Δ operator always applies at the point i, j, k; although the space subscripts are usually omitted to simplify notation motion. The subscript on the operator denotes the coordinate direction along which the difference is to be taken and the superscript the order of that difference.

With all the derivatives replaced by finite differences and after multiplication through by δt, (7) becomes

$$\begin{aligned} m^{n+1} = m^n &- \left[\frac{\omega_0 \delta t}{2\delta p}\right] \omega^{\ell} \Delta_i m^{\ell} - \left[\frac{v_0 \delta t}{2R\delta\phi}\right] v^{\ell} \Delta_j m^{\ell} \\ &- \left[\frac{u_0 \delta t}{2R\delta\lambda}\right] \frac{u^{\ell} \Delta_k m^{\ell}}{\cos(\phi_0 - j\delta\phi)} + \left[\frac{K_1 \delta t}{(\delta p)^2}\right] \Delta_i^2 m^{\ell} \\ &+ \left[\frac{K_2 \delta t}{R^2(\delta\phi)^2}\right] \frac{\Delta_j(\cos(\phi_0 - j\delta\phi)\Delta_j m^{\ell})}{\cos(\phi_0 - j\delta\phi)} + \left[\frac{K_2 \delta t}{R^2(\delta\phi)^2}\right] \frac{\Delta_k^2 m^{\ell}}{\cos^2(\phi - j\delta\phi)} , \end{aligned} \tag{11}$$

where the n and n + 1 superscripts denote the base time level and the newly generated time level respectively, and the ℓ superscript, which also denotes time, can take on only one or the other of these two values.

Each of the factors in brackets in (14) is the product of δt with a collection of constants which, when combined, has the units of reciprocal time. Thus each bracket forms the dimensionless ratio of the timestep to a time characteristic of the particular process changing the mixing ratio. For example, in the first term $2\delta p/\omega_0$ represents the vertical advection time or in the fourth term $(\delta p)^2/K_1$ is the meridional diffusion time.

Since each of these factors is a constant, (11) is simplified by replacing them with single quantities to reproduce the simpler form

$$m^{n+1} = m^n - b_1\omega^\ell \Delta_i m^\ell - b_2 v^\ell \Delta_j m^\ell - [b_3/\cos(\phi_0 - j\delta\phi)] u^\ell \Delta_k m^\ell + b_4 \Delta_i^2 m^\ell + [b_5/\cos(\phi_0 - j\delta\phi)] \Delta_i \cos(\phi_0 - j\delta\phi) \Delta_j m^\ell + [b_6/\cos^2(\phi_0 - j\delta\phi)] \Delta_k^2 m^\ell \qquad (12)$$

The pressure increment is 12.5 mb, that of latitude 5° and that of longitude 10°. With this information the first three advection times are evaluated to give:

$$\tau_1 = 2\delta p/\omega_0 = 5 \text{ days}, \quad \tau_2 = 2R\delta\phi/v_0 = 1.25 \text{ days}, \quad \tau_3 = 2R\delta\lambda/u_0 = 2.5 \text{ days}. \qquad (13)$$

The value of τ_3 does not represent the actual advection time entering into the calculation since a factor of $\cos\phi$ is not included in its evaluation. This factor represents the decrease in advection time as the distance corresponding to $\delta\lambda$ shrinks with approach to the pole. Since the cosine of the latitude varies from .819 at 35 N to .087 at 85 N the actual zonal advection time changes by nearly an order of magnitude over the region of integration.

Since a state of nearly total ignorance exists with regard to the actual magnitudes of the eddy diffusivities in the stratosphere, the diffusion time along a given axis is set to a simple multiple of the advection time along the same axis. In this study the multiple (called $1/b_7$) is chosen to be eight. This means that the parameterized diffusion can remove departures from equilibrium 1/8 as fast as advection operating by itself. This assumption leads to the following values for the diffusion times:

$$\tau_4 = 40 \text{ days}, \quad \tau_5 = 5 \text{ days}, \quad \tau_6 = 20 \text{ days}. \tag{14}$$

The difference of a factor of four between τ_5 and τ_6 arises because $\delta\lambda = 2\,\delta\phi$ and, since the horizontal diffusion is assumed to be isotropic, the transport must occur four times as rapidly over half the distance.

The values of K_1 and K_2 corresponding to τ_4 and τ_5 are 1×10^4 cm^2 sec^{-1} and 4.5×10^8 cm^2 sec^{-1} compared to 2×10^4 and 1×10^{10} used in Prabhakara's parameterized study. That author's definition of diffusion and the one used here are essentially different. In the former case the diffusion was used to simulate transfer by the large-scale eddies, while in this study it has only to account for transfer by fluctuations too small to be represented in synoptic-scale data. The similarity between the two vertical diffusivities is unfortunate; one would have preferred to use a vertical diffusivity that differed from that of Prabhakara by a factor of at least ten because, in the parameterized studies, diffusion is called upon to provide much of the transport that advection accomplishes in this model.

The entire treatment of diffusion is rather artificial but since it serves as a computational smoother, its effect can not be minimized without sacrificing numerical stability.

B. TIME INTEGRATION

Integration in time is accomplished using a backward corrected Euler scheme (see Kurihara, 1965). If the advective and diffusive terms in (12) may be replaced by $f(m^n, {}^n, v^n, u^n)$ this scheme may be represented thus:

$$m^{\ell} = m^{n} + f(m^{n}, \omega^{n}, v^{n}, u^{n}), \tag{15}$$

$$m^{n+1} = m^{n} + f(m^{\ell}, \omega^{n+1}, v^{n+1}, u^{n+1}). \tag{16}$$

Given the field of m^n and the wind at the n time level m^{ℓ} is computed from (15). Then m^{ℓ} and the winds at the n + 1 time level are used in (16) to obtain m^{n+1}. Thus m^{n+1} is first predicted using a forward difference and then corrected with a backward difference, the entire process being repeated at each successive time level until m is known for the entire period of interest.

According to Kurihara (1965), if this method is applied to the one dimensional advection equation,

$$x^{\ell} = x^{n} + b\Delta_i x^{n} \tag{17}$$

$$x^{n+1} = x^{n} + b\Delta_i x^{\ell} \tag{18}$$

stability will result for $b \leq 1$. By experiment, it was discovered that optimum results are obtained by using a time step δt = 1/48 day producing the following values for the b's (b_7 = 1/8)

$$b_1 = 4.17\times10^{-3},\quad b_2 = 1.67\times10^{-2},\quad b_3 = 8.33\times10^{-3}$$
$$b_4 = 0.52\times10^{-3},\quad b_5 = 4.17\times10^{-3},\quad b_6 = 1.04\times10^{-3} \tag{19}$$

These values are obviously much less than one, but the factor of $1/\cos\phi$ makes the coefficient of the third term much larger near the pole. At

80 N, the most northerly point at which (15) and (16) are applied, cos = .174 so $b_3/\cos$ = 0.047 still well within the region of stability. Unfortunately, a longer time-step drastically reduces the quality of the results and, although no theoretical investigation is attempted, this may be caused by either mass imbalances in the wind data or by the variability of the space increment resulting from the cosϕ effect.

C. WIND DATA

The wind data used by Mahlman (1967, 1969) are employed in the advective terms of (11). The data, which cover the 41 day period from 15 November until 25 December 1958, consist of the three wind components and the fields of temperature and geopotential height tabulated at 50 and 100 mb for the region from 40 to 80 N. Originally the two horizontal wind components as well as the temperature and height fields were extracted directly from the Weather Bureau (1963) stratospheric daily chart series for the IGY, while the ω's were computed from the other fields using the thermodynamic equation with an assumed diabatic heating rate (Mahlman, 1967).

During the early portion of the period of data coverage, the polar night vortex is intensifying with the circulation dominated by a cold low over northern Asia. Then on 21 November the flow undergoes a pulsation or "minor breakdown", becoming more meridional in character and remaining disturbed until 11 December when the vortex re-stabilizes with an important wave number two component. During this last period one trough lies over Asia and the other over North America with the two intervening ridges over the oceans.

With the exception of the ten-day period from 5 December until 15 December, the mean cell in these data has rising motion over the pole and descent in middle latitudes (Mahlman, 1969). Even during the time in December when the vertical motion reverses at the pole, descent takes place only in the immediate region of the pole with rising motion continuing in the 60 to 70 N band. This means that, except for that brief period in December, the mean cell oeprates in the exact opposite sense to that required by the Brewer-Dobson theory.

Unfortunately, the data are tabulated every 24 hours, on only two pressure surfaces, and for a somewhat coarser horizontal grid. This means that the data have to be extended by extrapolation and interpolation in both space and time. First, using the thermal wind equation, the horizontal winds are extrapolated upward to 12.5 mb and downward to 150 mb, and the ω's at these two levels are assumed to be zero. This is done at every point in the horizontal that carries the initial data fields (every 40° of longitude at 80 N, every 20° at 70 N, and every 10° of longitude at 50, 50 and 40 N). Values for every 10° longitude at 70 N 80 N are generated by linear interpolation between the tabulated values and the same process is applied again to produce winds at odd multiples of five degrees of latitude. Finally, a cubic Lagrange interpolating polynomial is fitted to the data at each horizontal grid intersection for the four levels and evaluated at the intermediate pressure levels to complete the wind field for each day. The wind for each time step is obtained from the daily wind fields by simple linear interpolation in time.

The wind data require still more treatment before they are suitable for use in the integration scheme. Due to inaccuracies in observation

and processing, the probable errors in the v wind component are at least as large as the real mean cell. Furthermore, the omegas generated by the thermodynamic method are not necessarily consistent with the divergences of the horizontal wind. Mass imbalances in the large-scale eddies, while undesirable, tend to cancel each other when integrated over the entire region, but a mean cell with spurious mass sources may seriously distort the results of the computation. It was decided to remedy the situation by removing the natural mean cell and replacing it with an artificial time independent one which exactly satisfied the zonally-averaged continuity equation. The following transformation accomplishes this end:

$$
\begin{aligned}
u''^{\ell}_{i,j,k} &= u^{\ell}_{i,j,k} \\
v''^{\ell}_{i,j,k} &= v^{\ell}_{i,j,k} - \tilde{v}^{\ell}_{i,j} + V^{\ell}_{i,j} \\
\omega''^{\ell}_{i,j,k} &= \omega''^{\ell}_{i,j,k} - \tilde{\omega}^{\ell}_{i,j} + \Omega^{\ell}_{i,j} \quad .
\end{aligned}
\tag{20}
$$

Here the double primed quantities are the new values, the unprimed the old, the tilded the zonal mean old values, and the capitals the contrived mean. This new mean is usually run with ascent at the poles; although some experiments were run with the cell reversed for comparison. Typical magnitudes for the new mean were on the order of a knot for V and .5 mb day^{-1} for Ω. The new cell was constant in time and no attempt was made to introduce time variations resembling those of the natural mean cell.

While use of an artificial mean cell seems to introduce the very element of arbitrariness that was avoided through employing observed winds, it should be pointed out that this approach both permits experimentation with mean cells of differing character and allows use of mean circulations that are more or less consistent with heat and momentum considerations.

III. EXPERIMENTS

A. OZONE SIMULATION

1. Boundary and Initial Conditions

The behavior of stratospheric ozone is simulated by the evolution of an inert tracer from a zonally symmetric initial state roughly corresponding to the observed zonal mean ozone distribution (Hering, 1960). Throughout the integration the observed initial values at 12.5 and 150 mb are retained at the top and bottom boundary points. This condition can be justified since it is assumed that the value at 12.5 mb is controlled only by photochemistry and is time-independent except for diurnal and seasonal variation which are not reproduced. Similarly the mixing-ratio at 150 mb is assumed to represent a constant equilibrium between downward transport and destruction in the troposphere.

Originally it was the intention to parameterize advection into the region from the tropics by retaining the observed zonal mean values at the southern boundary points, but the final version of the model is permitted to generate its own southern boundary condition inasmuch as the points at 35 N are all set to the generated zonal mean of those at 40 N.

Near the pole, the cosine of the latitude becomes small causing an apparent singularity in the prognostic equation. This difficulty can be avoided by applying a cartesian version of the prognostic equation at the pole, but a simplier solution is suggested by the treatment of the southern boundary, so the values at 85 N are set to the zonal mean of those at 80 N.

These boundary conditions imply that the system is not closed since boundary fluxes can occur through all surfaces of the region of integration. A horizontal flux through the southern boundary is physically reasonable since advection from tropical regions is an important source of mid and high-latitude ozone. Similarly, the flux over the pole is to be expected; although the boundary scheme used does not properly simulate it, and a spurious over-the-pole transfer arises which distorts the final results. The upper boundary condition allows ozone to be transported downward into the region of integration but does not permit it to leave through the top. The values at 12.5 mb are invariably higher than those in the interior of the region. Since the vertical motion is small near the upper boundary, diffusion predominates allowing the tracer to flow inward but never outward. A similar set of conditions arises at the lower boundary; except here the boundary values are always lower than those in the interior so only outward fluxes can occur. Thus, although no source of sink terms are explicitly included in the model, the boundary conditions crudely approximate the behavior of photochemical sources in the upper stratosphere with a sink at the tropopause.

2. Results

Figures 1 through 5 are a series of charts portraying the ozone mixing ratio and geopotential height on the 50 and 100 mb levels at intervals of 5 days during the period of integration. Comparison between the 50 mb and 100 mb pressure levels indicate that the degree of continuity of the ozone field between these two levels is comparable to that observed in the geopotential height field so that representation of more than one horizontal section of the ozone field is superfluous, and only the 100 mb surfaces are presented after 25 November.

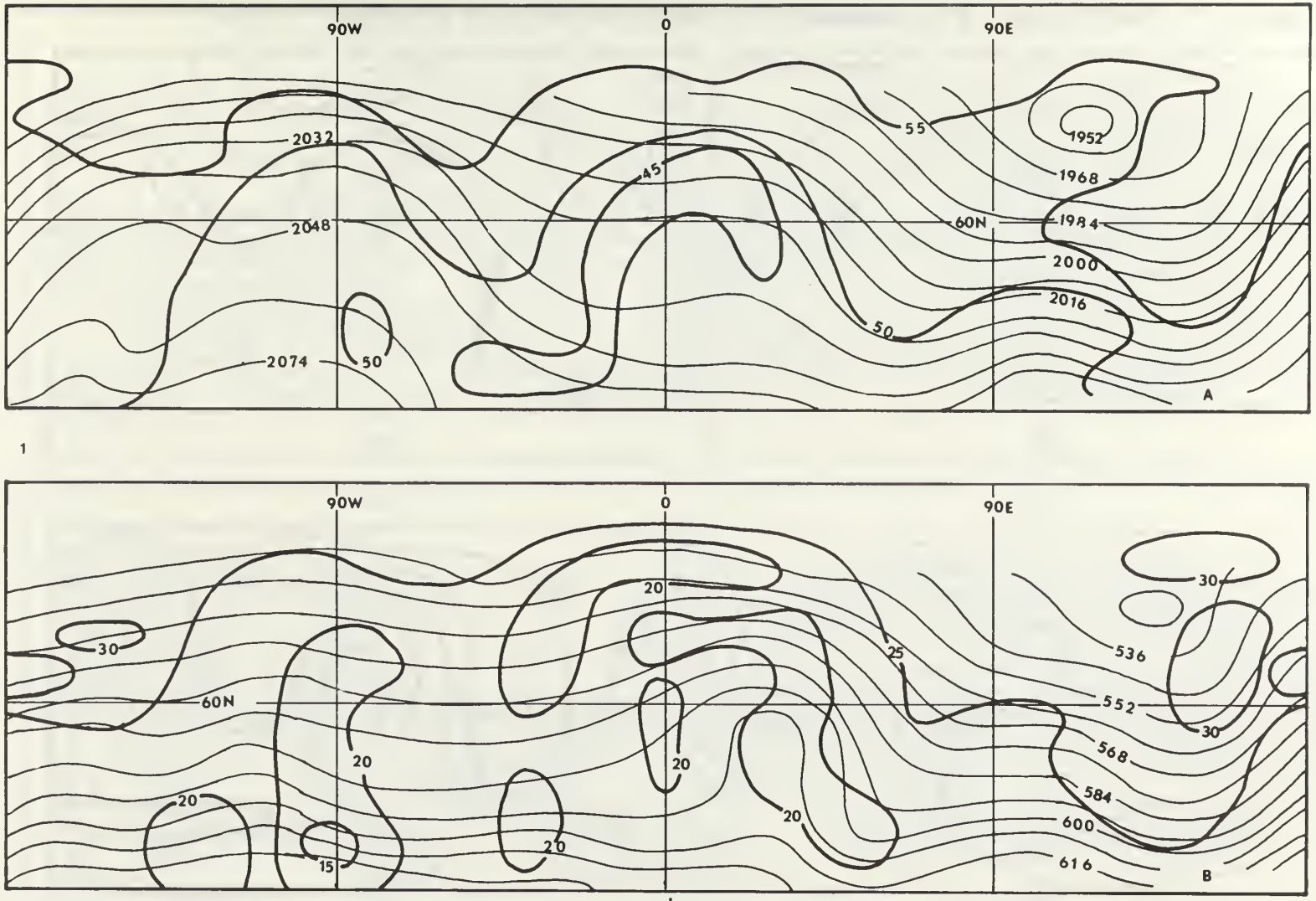

FIG. 1. Simulated ozone mixing ratio in gm-gm^{-1} on 20 November at pressure altitudes of A: 50 mb; and B: 100 mb. Heavy lines are the mixing ratio contours while the lighter lines are jeopotential height contours.

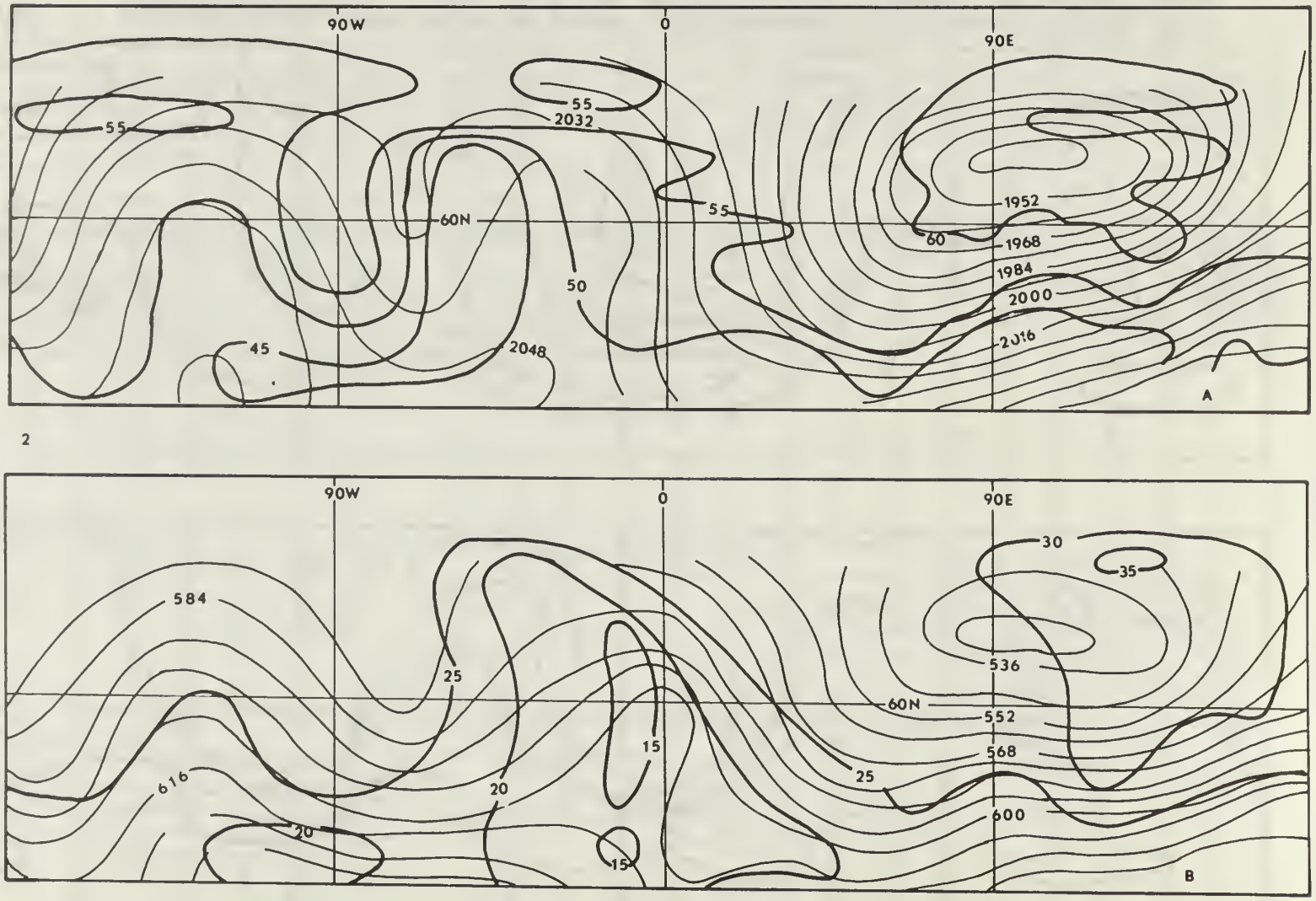

FIG. 2. Simulated ozone mixing ratio on 25 November at A: 50 mb; and B: 100 mb.

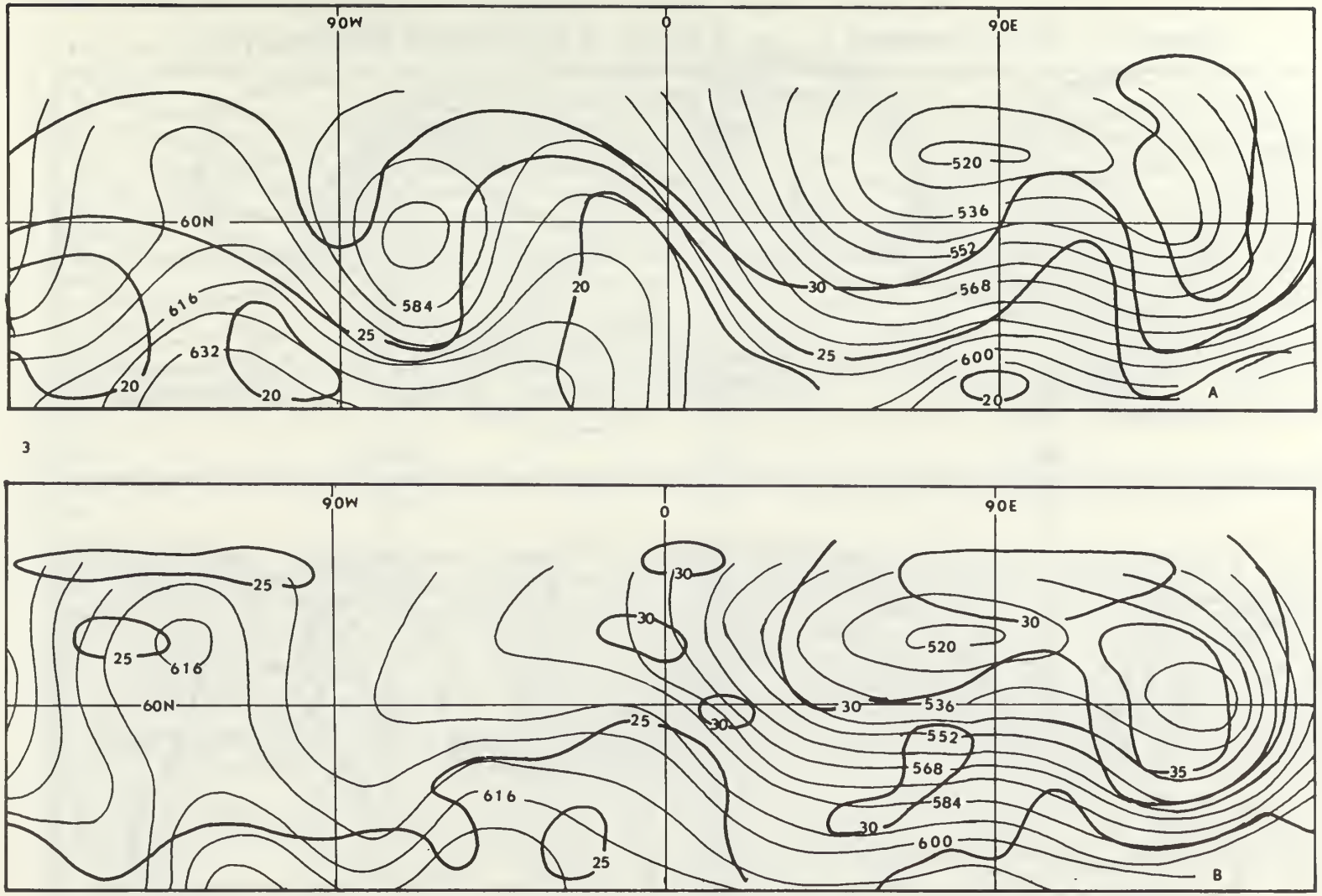

FIG. 3. Simulated ozone mixing ratio at 100 mb on A: 30 November; and B: 5 December.

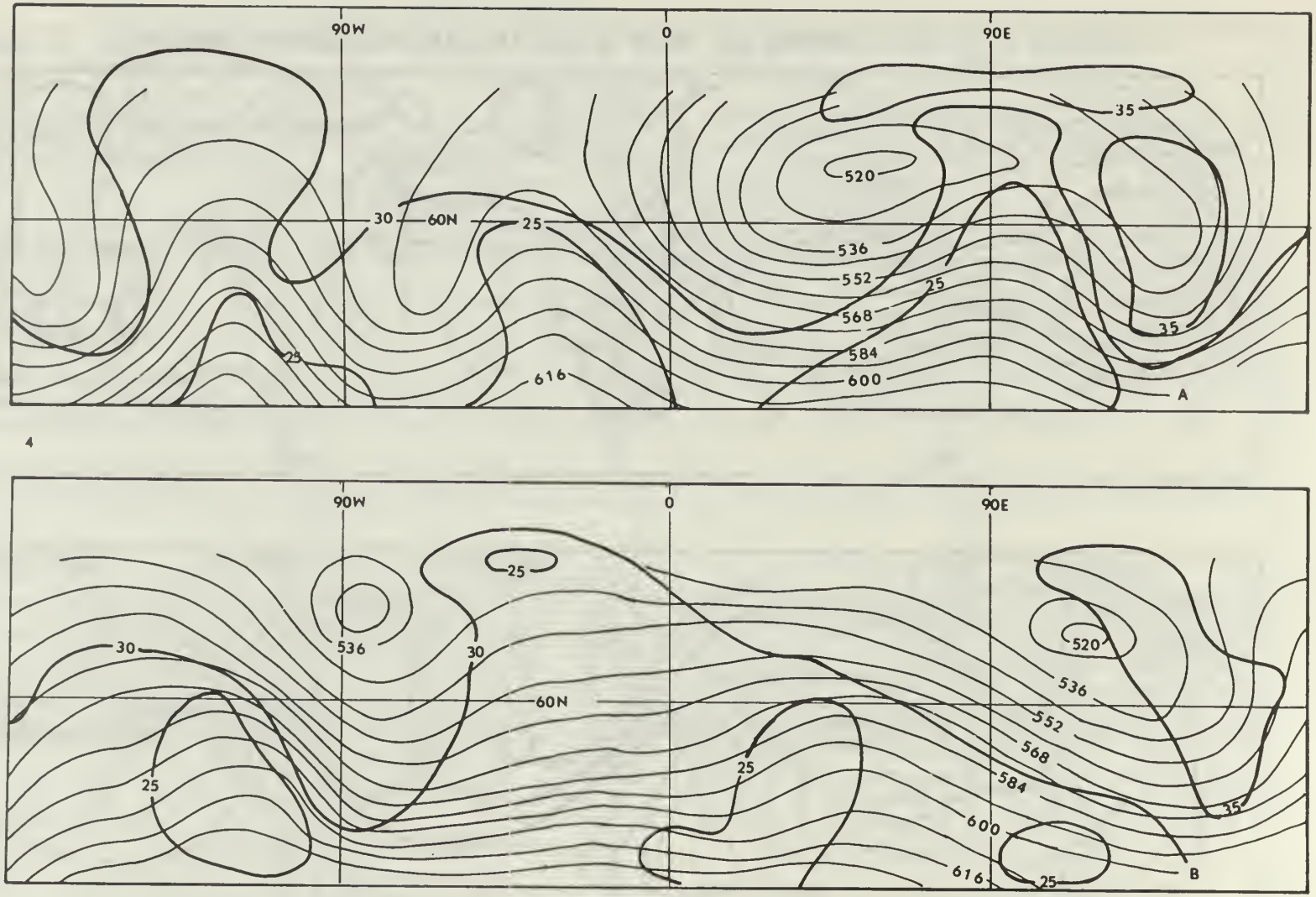

FIG. 4. Simulated ozone mixing ratio at 100 mb on A: 10 December; and B: 15 December.

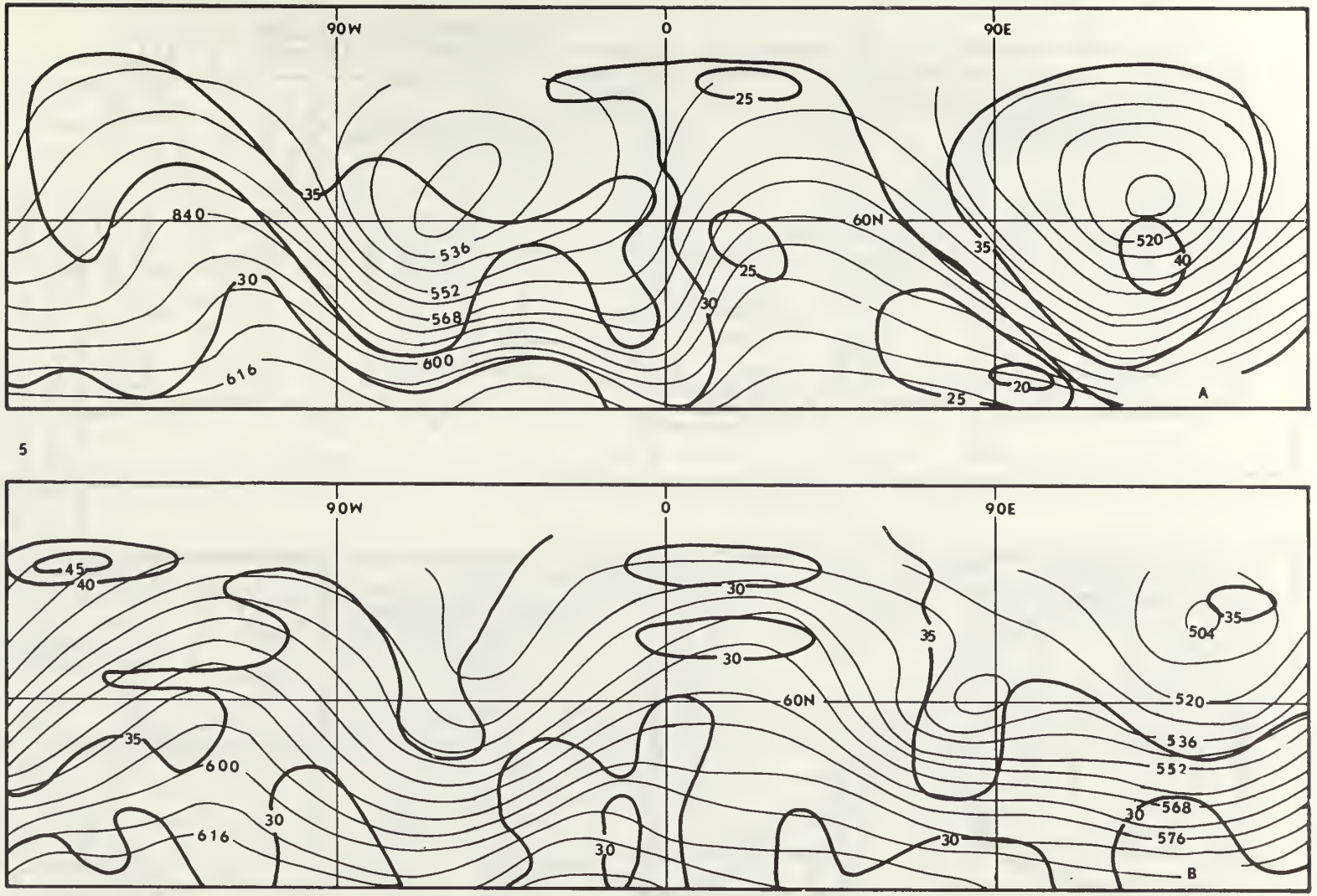

FIG. 5. Simulated ozone mixing ratio at 100 mb on A: 20 December; and B: 25 December.

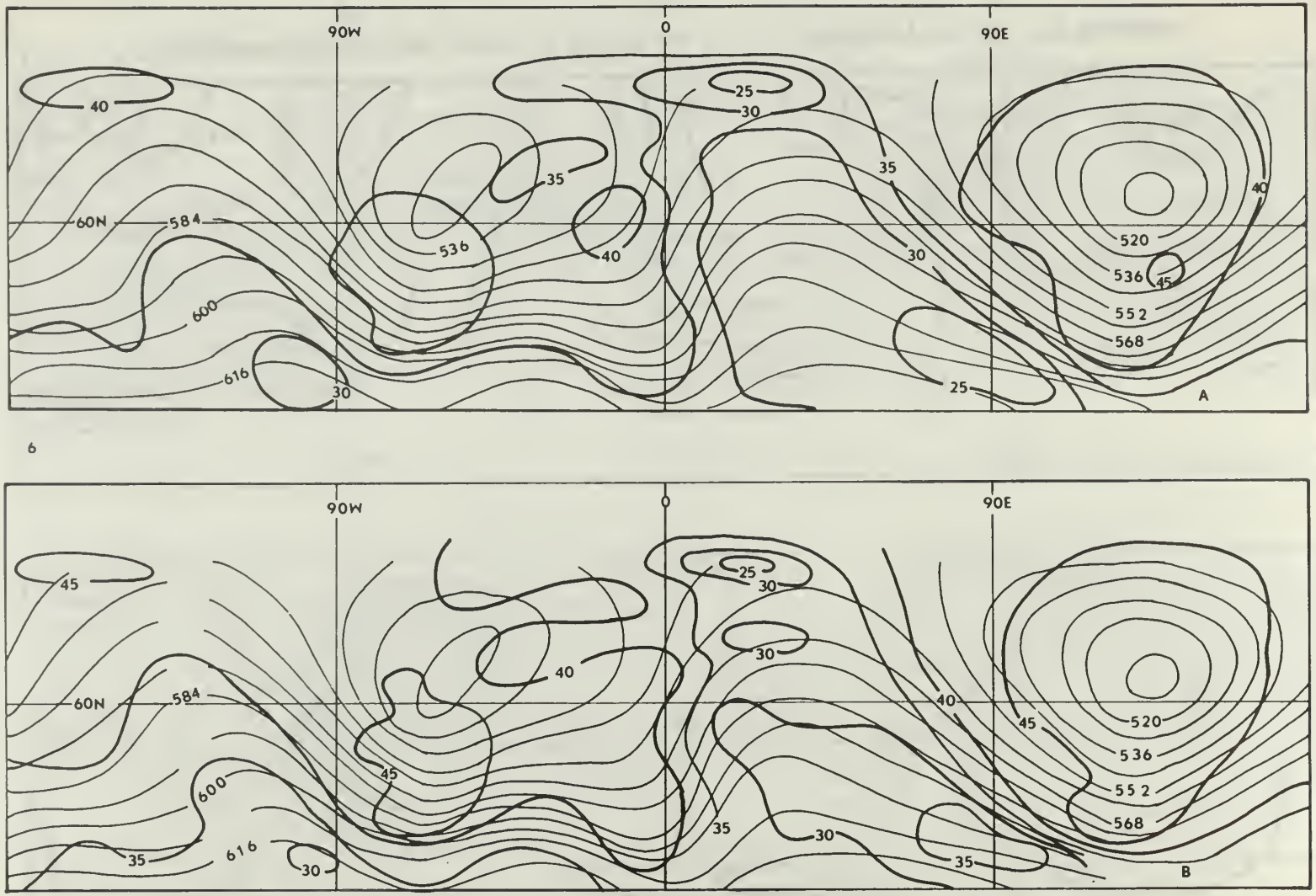

FIG. 6. Simulated ozone mixing ratio on 20 December for A: reverse mean cell; and B: zero mean cell.

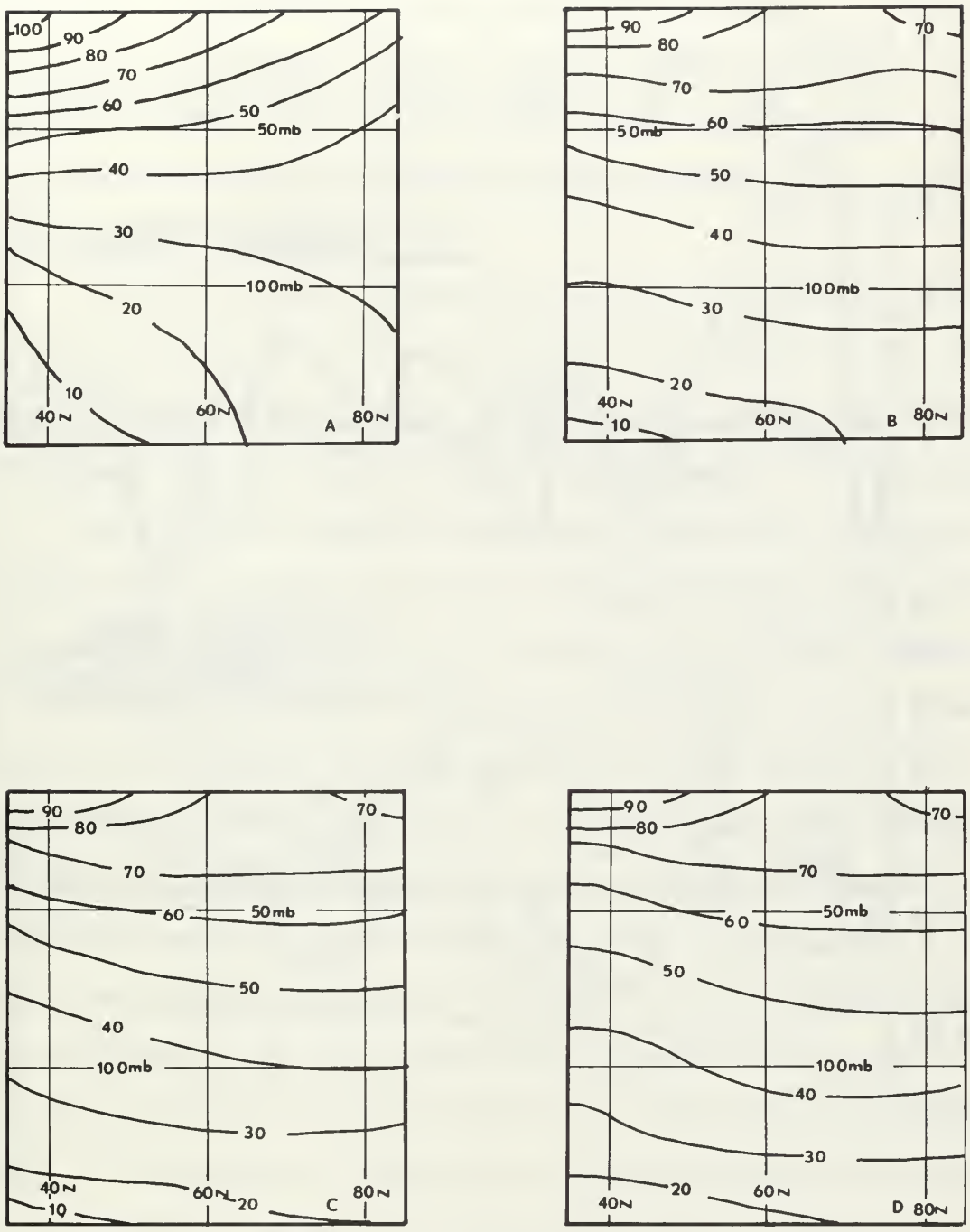

FIG. 7. Simulated zonal-mean ozone cross section in μgm-gm^{-1} A: Initial cross section; B: cross section for 20 December with mean ascent at the pole; C: for the same date with a zero mean cell; and D: for a mean cell with descent at the pole.

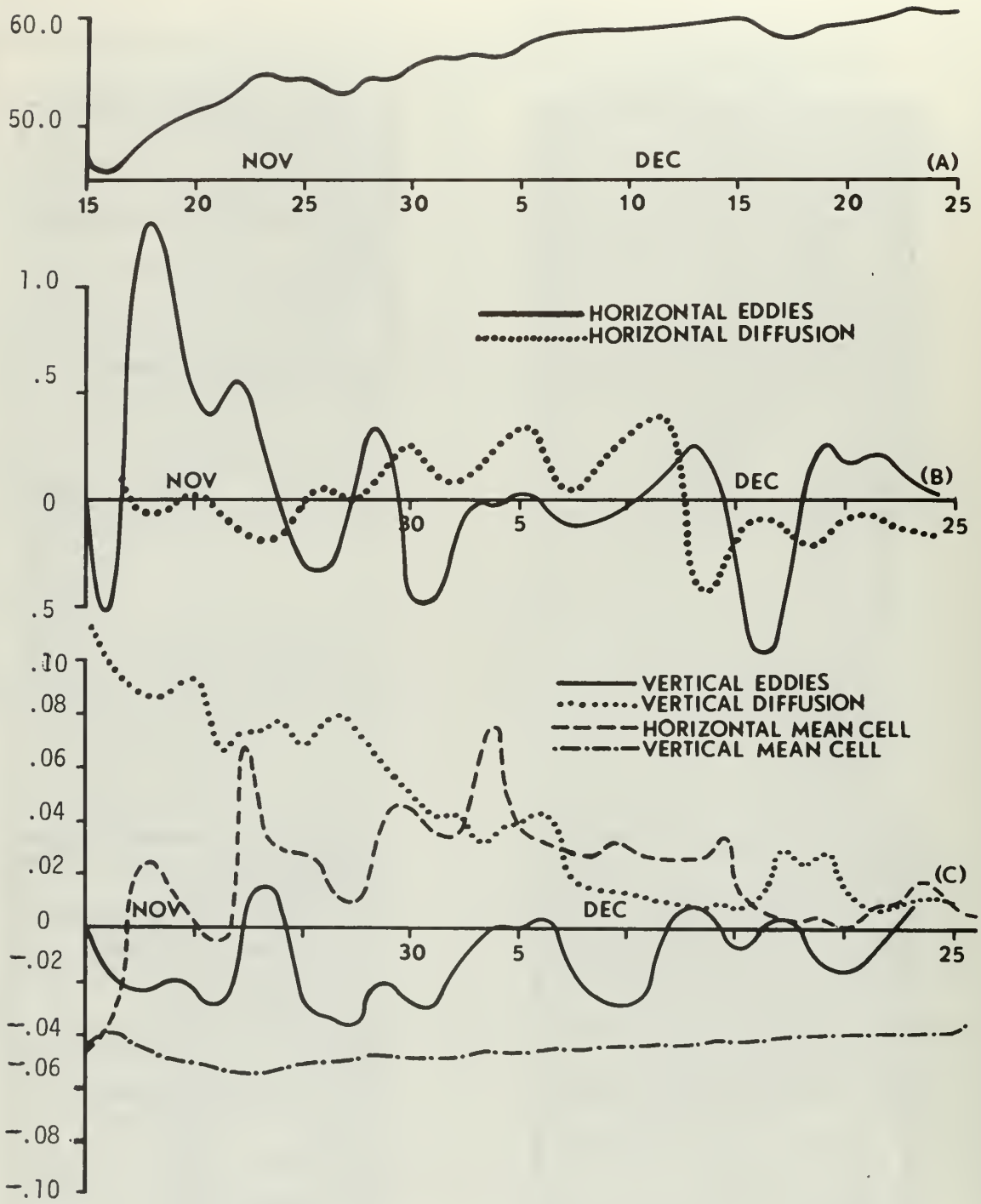

FIG. 8. A: Simulated zonal-mean ozone mixing-ratio at 60 N and 50 mb as a function of time; B: the effect in μgm-gm^{-1} day^{-1} of the horizontal eddies and diffusion on the zonal-mean mixing-ratio at 60 N and 50 mb as a function of time; and C: the effect of the horizontal mean cell, and the vertical eddies, diffusion and mean cell in the same units.

These charts show a number of qualitative features that are reassuringly similar to the characteristics of the real atmospheric ozone field. Dobson's (1924) observations of ozone maxima in the troughs are reproduced. Similarly, Bozkov's (1968) observations of sinusoidal isopleths of concentration with ozone maxima in the standing troughs over continents and minima over the intervening seas appear in these fields.

At 50 mb and 60 N the normalized correlation coefficient between ω and m, computed over the entire period of integration, is 0.22. This means that the high mixing ratios in the lows can be explained in terms of advection from above just as Reed (1950) and Normand (1953) postulated.

On the 50 mb surface the ozone mixing ratio values initially decrease from .053 μgm/gm at 35 N to 0.028 μgm/gm at 85 N while at 100 mb the initial values increase from 0.010 to .031 in the same interval. As the integration proceeds the transport processes reverse the 50 mb gradient by 18 November and establish a mid-latitude maximum at 75 N by 25 November. This maximum tends to drift southward appearing most frequently at about 65 N during the latter portion of the experiment. It is quite persistent in this latitude, but often it disappears for several days, being absent on a total of 19 of the 41 simulated days. A similar maximum appears in the 100 mb profile on 2 December but it is less pronounced and not nearly so persistent in time (being present on 10 of 41 days). At both altitudes the maximum zonal mean gradient occurs south of the latitude of maximum mixing ratio, with the field being more nearly flat over the pole. These results are consistant with Bozkov's work, and since they arise during the integration and do not represent more persistence of the initial state, they enhance confidence in the model.

When time series of the zonal mean mixing ratio and of the various processes modifying it are considered (see FIG. 8), it is found that the horizontal eddies and horizontal diffusion are very highly correlated with the fluctuations of the mixing ratio. The other processes, the vertical eddies, the vertical and horizontal mean cells and the vertical diffusion are all about an order of magnitude smaller than these first two effects and did not produce noticable, short-term changes in the mixing ratio.

The direction of horizontal eddy transport changes during the integration. At the beginning it is poleward, but during the pulsation of the polar night vortex it changes sign and remains negative for 22 days until the vortex begins to re-intensify. When the normalized mixing-ratio and meridional velocity correlation coefficient is computed for the entire period, its value is + .023 at 50 mb and 60 N. But when the data are stratified into poleward and equatorward transport periods, the correlation during the former is + .317 and the latter -.237. Since the omega-mixing-ratio correlation is + 0.22, this indicates that the difference in the effectiveness between the vertical and horizontal eddies is primarily caused by the smaller ratio of characteristic velocity to space increment for the former.

Because the mean cell is constant in time and the zonal mean gradient is nearly so, the sign and magnitude of the instantaneous change resulting from the mean cell is quite persistent. This means that, while the short-term effect is small, the mean cell produces a marked change in the field when integrated over 41 days.

This effect is well illustrated by the differences among the 20 December 100 mb fields in FIG. 5 and FIG. 6. Figure 6 shows the 20

December mixing-ratio field resulting from a zero mean cell as well as that resulting from a reversed mean cell. Comparison among these three charts indicates that in all cases the features are very similar in shape and location but the values differ as though the fields were translated by addition of a constant. This is very nearly what happened. Figure 7 shows the zonal mean cross sections for each of these three cases on 25 December as well as the initial zonal mean. Each different mean cell changes the inclination of the mixing ratio isopleths, tending to increase their slopes when sinking occurs at the pole and decrease them when rising takes place at the pole. This effect is most important in the northern portions of the region where it moves the lines in the vertical while toward south they remain at about the same altitude in all cases. It should be pointed out that, while this effect becomes important only after long integration times, it will eventually attain an equilibrium with the other processes and not accumulate indefinitely.

Apparently the model seeks to attain just such an equilibrium during this simulation. At 50 mb and 60 N the mixing ratio rises asymptotically to a value of about 60 $\mu gm/gm^{-1}$ (See FIG. 8). The horizontal eddies, the vertical diffusion, and the horizontal mean all appear to contain decaying transients that largely damp out by 10 December. Thus, apparently about 25 days are required to recover from the dis-equilibrium introduced when the model is initiated from a zonally symmetric initial state.

The contribution of both components of the sub-grid-scale diffusion is disturbingly large. This phenomenon is dependent upon a completely arbitrary sub-grid-scale parameterization scheme and probably is much stronger than any real atmospheric diffusion. It is unfortunate that

the diffusivities can not be reduced without impairing the model's computational properties. The un-naturally strong diffusion may mask important advective processes and spuriously shorten the equilibrium time as well as displace the equilibrium from its true value.

B. RADIOACTIVE DEBRIS SIMULATION

1. Boundary and Initial Conditions

Clouds of radioactive debris are simulated by permitting the distribution of tracer to evolve from an initial three dimensional Gaussian distribution centered at a point within the region of integration. It would be more satisfying to use an initial state in which all the tracer is concentrated at a single grid point, but in such experiments an undesirable computational mode is excited by the steep gradients so that the results are meaningless.

The boundary conditions imposed upon the evolving cloud of debris represent a serious problem. For the previous experiment with zonally symmetric ozone fields as an initial state, the generated zonal mean of points along the next interior latitude circle represents a reasonable boundary value. Because the point source problem is asymmetrical, constraining the gradient at the southern boundary to zero seems to constitute a reasonable boundary condition, but computational difficulties arise in this case when the wind normal to the boundary is strong. The final solution to this problem lies in a compromise between the two approaches. Each boundary point at 35 N or 85 N is set to a weighted average of the zonal mean at the next interior parallel and the value at the adjacent point along that parallel. The weighting factors are 0.7 times the mean and 0.3 times the adjacent point at the southern boundary, and equal weights are used at the northern boundary.

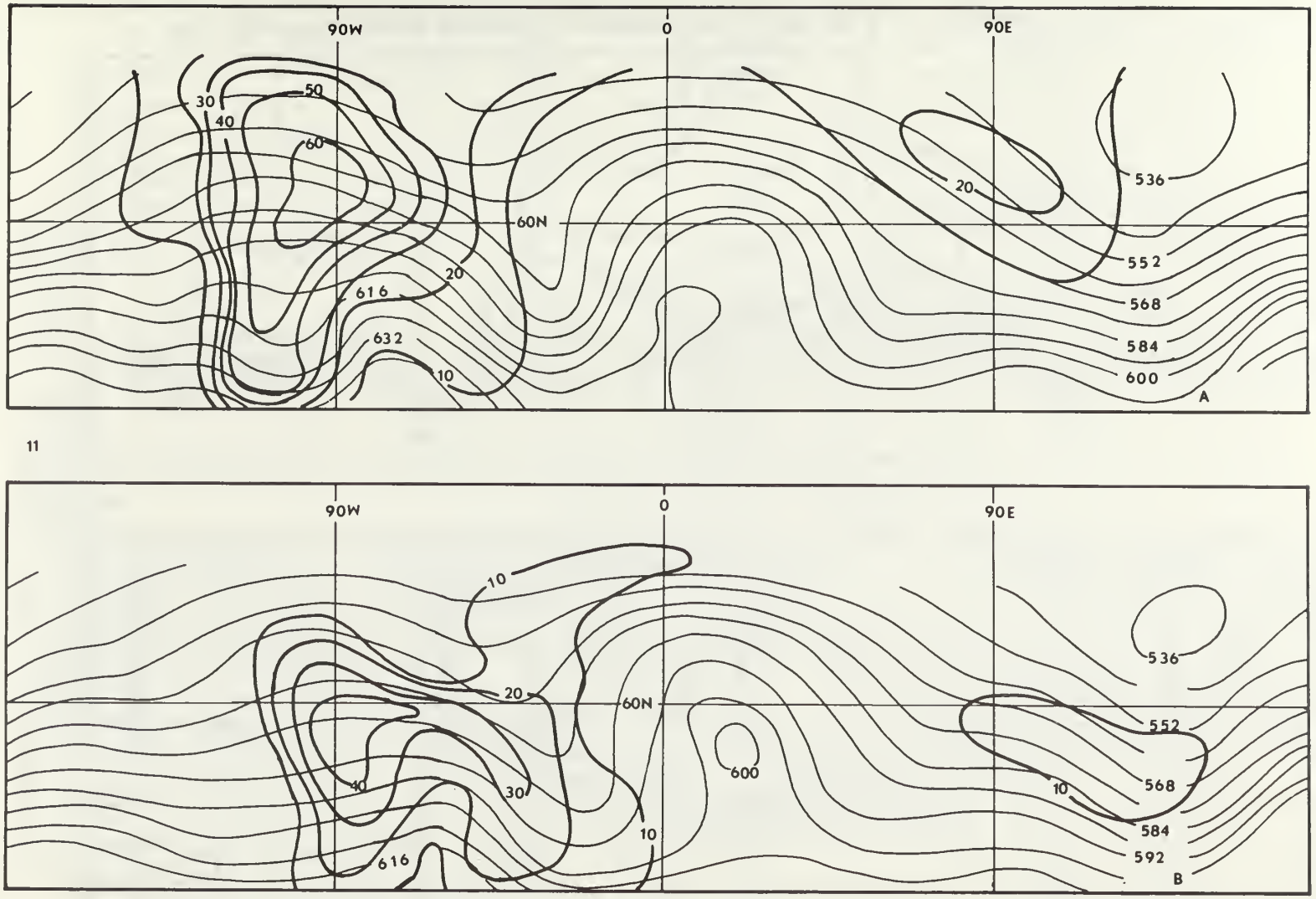

FIG. 9. Simulated radioactive debris distribution at 100 mb in arbitrary units on A: 18 November; and B: 20 November. The heavy lines are the mixing ratio contours while the light lines are the geopotential height contours.

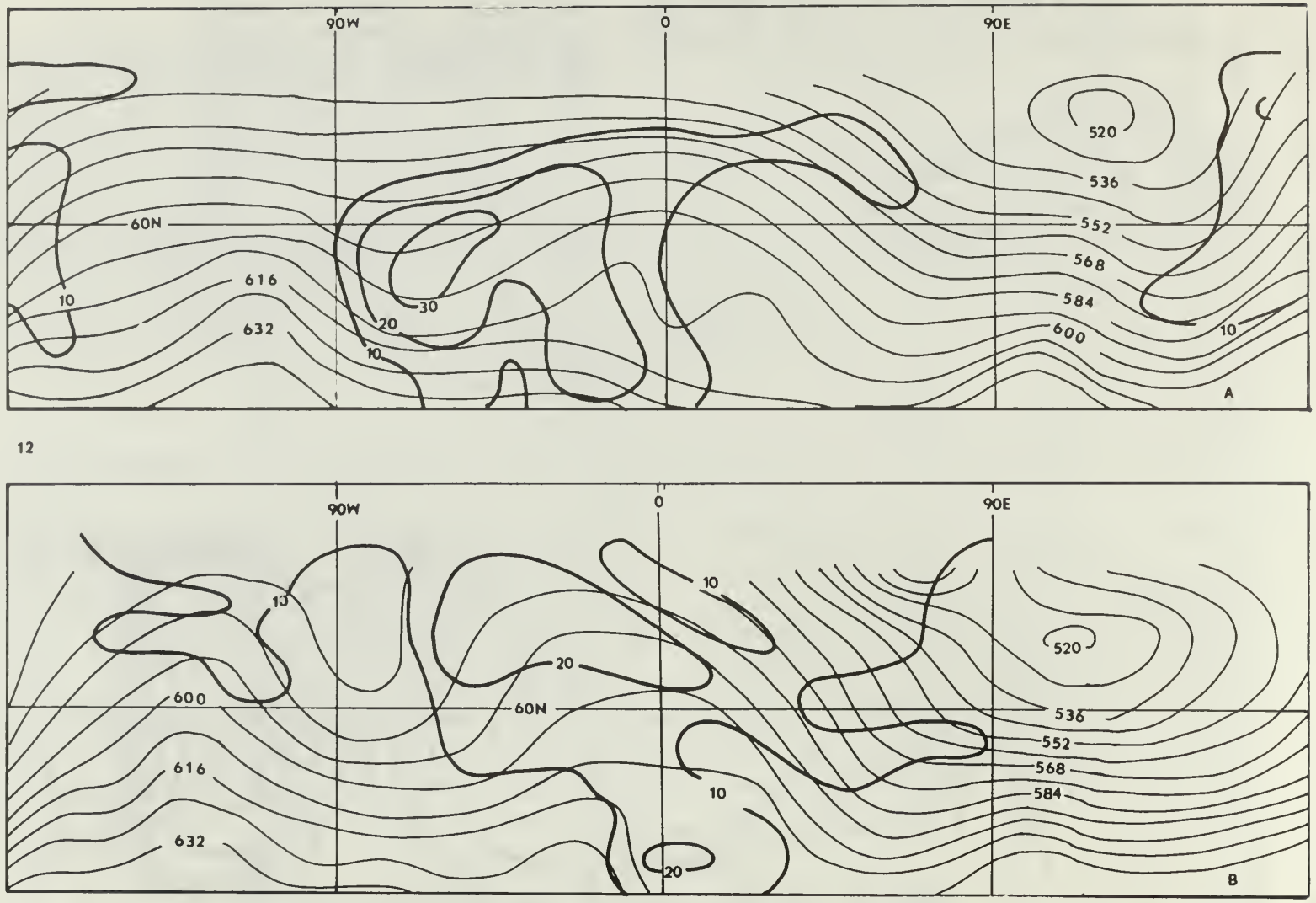

FIG. 10. Simulated radioactive debris at 100 mb on A: 22 November; and B: 24 November.

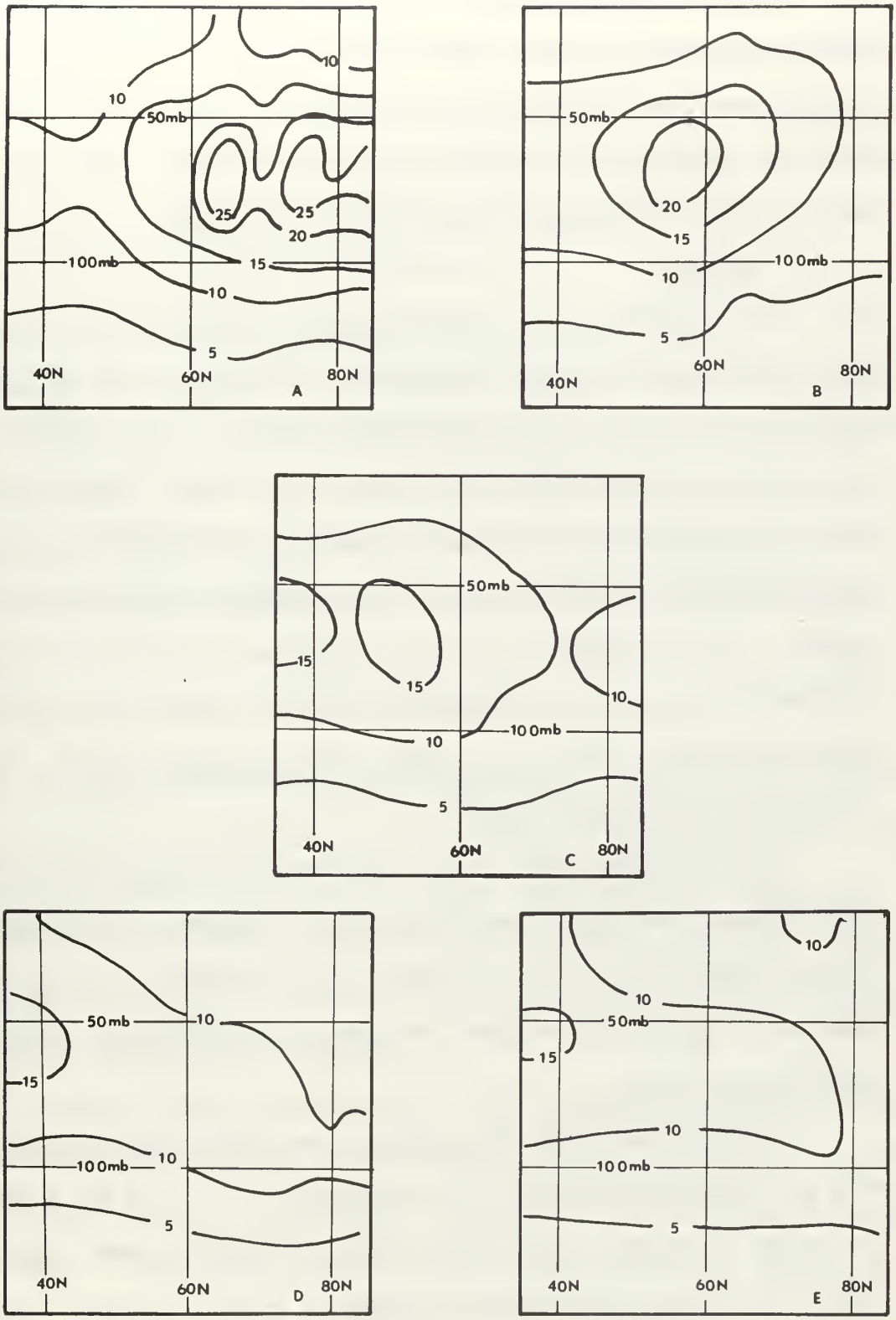

FIG. 11. Zonal-mean simulated radioactive debris in arbitrary units on A: 18 November; B: 20 November; C: 22 November; D: 24 November; and D: 26 November.

At the top and bottom of the region there is little inflow or outflow because the vertical velocities are small. Furthermore, these regions are fairly remote from the centers of concentration. This means that zero gradient at 12.5 and at 150 mb constitutes a physically reasonable and numerically stable boundary condition there.

2. Results

The evolution of a cloud injected at latitude 60 N longitude 140 W with initial standard deviation 10° of latitude, 20° of longitude and 25 mb of pressure was simulated for eleven days (See FIGS. 9, 10). This initial position lies in the almost purely zonal flow in the ridge over the Northern Pacific so that the main mass of debris is carried eastward along the height contours while gradually spreading and dispersing. By 23 November the cloud has migrated about 90° of longitude and lies in the eastern portion of the Atlantic ridge. During this period the mixing ratio at the last closed contour decreases from 80, its initial value, to 20 (arbitrary units).

On 17 November part of the cloud is carried over the pole and then southeastward around the Siberian low. Between 19 and 21 November the mass rounds the trough and begins to move northward so that by 23 November it has circumnavigated the pole at high latitudes and re-merged with the main cloud.

In the zonal mean, the center of the initial distribution lay at 60 N and a pressure altitude of 75 mb (See FIG. 11). As the cloud evolves the center of maximum mixing ratio gains altitude and moves toward the south, at the same time spreading laterally in such a manner that its axis slopes downward toward the pole. By 23 November the zonal mean bears a striking resemblance to both the results of parameterized studies

and to observations (Gudiksen et al., 1969), showing that this model can, through advection and diffusion alone, quickly shape any reasonable distribution of inert tracer into a fair reproduction of observed mixing ratio fields. In fact, this process took place much more quickly than it would have in the real atmosphere because of the large standard deviation in the initial distribution.

No detailed analysis is made of the principal agencies responsible for the tracer's evolution, but the horizontal eddies and diffusion combined are about an order of magnitude stronger than the sum of the other four agencies. However, as in the ozone experiments, the sign of the tendencies produced by the mean cell terms remain consistent in time so that over periods longer than eleven days their effect becomes significant.

IV. CONCLUSIONS

This model successfully simulates many observed qualitative features of stratospheric transports of both ozone and radioactive debris. Apart from some numerical difficulties which result from mass imbalance in the wind field and from inadequate treatment of the singularity at the pole, no obstacles exist to prevent the use of this model to predict the evolution of stratospheric tracers.

If the erroneous exaggeration of the parameterized diffusion may be neglected, the instantaneous derivative is primarily determined by the horizontal eddies. Although the effect of the vertical eddies is about an order of magnitude weaker than that of the horizontal eddies, it cannot be neglected in the zonal mean. The two components of the mean cell are still weaker than the vertical eddies. However, over long periods of time, they may assume greater importance because they do not change sign or fluctuate greatly in magnitude.

BIBLIOGRAPHY

Bozkov, D., 1968: Planetary distribution of total ozone during IQSY. Khidrologiia i Meteorologiia, 23, 29-39.

Brewer, A. W., 1949: Evidence for a world circulation provided by measurements of helium and water vapor distributions in the stratosphere, Quarterly Journal of the Royal Meteorological Society, 75, 351-363.

Craig, R. A., 1965: The Upper Atmosphere, Meteorology and Physics. Academic Press, 509 pp, 200-208.

Davidson, B., Friend, J. P. and Seitz, H., 1965: Numerical models of diffusion and rainout of stratospheric radioactive materials. Tellus, 18, 301-315.

Dobson, G. M. B., Harrison, D. N., and Lawrence, J., 1937: Measurements of the amount of ozone in the earth's atmosphere and its relation to other geophysical conditions. Proceedings of the Royal Society of London, Ser A, Part II, 114, 521-541.

Dobson, C. M. B., 1956: Origin and distribution of the polyatomic molecules in the air. Proceedings of the Royal Society of London, Ser A, 236, 187-193.

Godson, W. L., 1960: Total ozone and the middle stratosphere over Arctic and Sub-Arctic areas in winter and spring. Quarterly Journal of the Royal Meteorological Society, 86, 301-317.

Gudiksen, P. H., Fairhall, P. W., and Reed, R. J., 1968: Roles of mean meridional circulation and eddy diffusion in the transport of trace substance in the lower stratosphere. Journal of Geophysical Research, 73, 4461-4473.

Haltiner, G. J., and Martin, F. L., 1957: Dynamical and Physical Meteorology. McGraw-Hill, 454 pp, 244-247.

Hering, W. S., 1965: Ozone and atmospheric transport processes. Tellus, 18, 329-336.

Hunt, B. E. and Manabe, S., 1968: Experiments with a stratospheric general circulation model II. Monthly Weather Review, 96, 503-539.

Hunt, B. E., 1969: Experiments with a stratospheric general circulation model III. Monthly Weather Review, 97, 287-306.

Kurihara, Y., 1965: On the use of implicit and iterative methods for the time integration of the wave equation. Monthly Weather Review, 93, 33-46.

Mahlman, J. D., 1967: Further studies on atmospheric general circulation and transport of radioactive debris. Atmospheric Science Paper No. 110, Colorado State University, 68.

Mahlman, J. D., 1969: Energetics of a "minor breakdown" of the stratospheric polar night vortex. Journal of the Atmospheric Sciences, 26, (to be published).

Normand, Sir Charles, 1953: Atmospheric ozone and the upper air conditions. Quarterly Journal of the Royal Meteorological Society, 79, 39-50.

Newell, R. L., 1961: The transport of trace substances in the atmosphere and their implication for the general circulation of the stratosphere. Geophisica Pura e Applicata, 49, 137-138.

Prabhakara, C., 1963: Effects of non-photochemical processes on the distribution and total amount of ozone in the atmosphere. Monthly Weather Review, 91, 411-431.

Reed, R. J., 1950: Role of vertical motions in ozone-weather relationships. Journal of Meteorology, 7, 263-267.

Reed, R. J., and German, K. E., 1965: A contribution to the problem of stratospheric diffusion by large-scale mixing. Monthly Weather Review, 93, 313-321.

INITIAL DISTRIBUTION LIST

		No. Copies
1.	Defense Documentation Center Cameron Station Alexandria, Virginia 22314	20
2.	Library, Code 0212 Naval Postgraduate School Monterey, California 93940	2
3.	Naval Weather Service Command Washington Navy Yard Washington, D. C. 20390	1
4.	Asst. Professor Jerry D. Mahlman, Code 51Mz Department of Meteorology Naval Postgraduate School Monterey, California 93940	20
5.	LTJG Hugh Edward Willoughby, USN Airborne Early Warning Squadron ONE FPO San Francisco, Calif. 96637	1
6.	Dr. R. J. Engelmann Fallout Studies Branch Division of Biology & Medicine Washington, D. C. 20545	1

DOCUMENT CONTROL DATA - R & D

(Security classification of title, body of abstract and indexing annotation must be entered when the overall report is classified)

1 ORIGINATING ACTIVITY (Corporate author)
Naval Postgraduate School
Monterey, California 93940

2a. REPORT SECURITY CLASSIFICATION
Unclassified

2b. GROUP

3 REPORT TITLE
A Numerical Simulation of the Advective and Diffusive Transfer of Trace Substances in the Stratosphere

4 DESCRIPTIVE NOTES (Type of report and inclusive dates)
Master's Thesis, December 1969

5 AUTHOR(S) (First name, middle initial, last name)
Hugh E. Willoughby

6 REPORT DATE
December 1969

7a. TOTAL NO. OF PAGES
47

7b. NO. OF REFS
20

8a. CONTRACT OR GRANT NO.

b. PROJECT NO.

c.

d.

9a. ORIGINATOR'S REPORT NUMBER(S)

9b. OTHER REPORT NO(S) (Any other numbers that may be assigned this report)

10 DISTRIBUTION STATEMENT
This document has been approved for public release and sale; its distribution is unlimited.

11. SUPPLEMENTARY NOTES

12. SPONSORING MILITARY ACTIVITY
Naval Postgraduate School
Monterey, California 93940

13. ABSTRACT

A Numerical model which employs observed stratospheric winds to advect simulated tracers was developed. This model successfully reproduces many qualitative features of the observed fields of both ozone and radioactive debris. As the tracers evolve, the horizontal eddies constitute the principal process modifying the tracer zonal mean. Although the vertical eddies and the zonal mean cell are both an order of magnitude weaker than this process, the latter of these tends to always act in the same sense so that its effect becomes more important over long periods of time.

14 KEY WORDS	LINK A		LINK B		LINK C	
	ROLE	WT	ROLE	WT	ROLE	WT
Ozone						
Radioactive Fallout						
Advection						
Diffusion						
Numerical Simulation						
Stratosphere						